

# The effect of SiC decomposition on microstructure of Ni<sub>3</sub>Al

Ö. GÜLER\*, E. EVIN, O. YILMAZ, S. H. GÜLER

*Department of Metallurgy and Materials Engineering, Fırat University, Elazığ 23119, Turkey*

The intermetallic matrix composites (IMCs) of Ni<sub>3</sub>Al reinforced by SiC were fabricated by powder metallurgical routes via solid state reaction of nickel and SiC particulates by volume combustion process. Pure nickel, aluminum and SiC powders were used as initial substances. The powders were mixed, and the compacts were combusted in an atmosphere controlled furnace. The synthesis of the SiC added Ni<sub>3</sub>Al was attempted to improve the nature of the Ni<sub>3</sub>Al composite. The initially added SiC particles were unstable and decomposed partially within the matrix during combustion, and the morphology of the IMCs changed upon the dissolution rate of SiC and combustion temperature. It was confirmed that the dissolution rate of SiC was effective on improvement of the hot working temperature of Ni<sub>3</sub>Al IMCs.

(Received January 13, 2015; accepted June 24, 2015)

*Keywords:* Ni<sub>3</sub>Al, Intermetallics, Reaction sintering, Combustion synthesis

## 1. Introduction

Combustion synthesis represents an attractive technique for the preparation of intermetallics and a variety of other materials, including carbides, borides, nitrides, silicides, hydrides, composites, etc. [1-4]. Combustion synthesis of intermetallic compounds can be conducted in either of two modes, the self-propagating high-temperature synthesis (SHS) and the volume combustion (VC). The volume combustion conducts a gradual heating of the sample uniformly in a controlled atmosphere until the reaction occurs simultaneously throughout the entire sample. Temperatures of the reactions relate to the reaction synthesis, compaction of the raw materials, specific surface, and other processing parameters. The procedure has low energy consumption and has large potentials for industrial applications due to the high productivity and the simplicity of the equipment involved. In addition, synthesis and sintering could be made within only one-step [6]. Due to high temperatures and velocities of reactions, limited information is available on the mechanism and on the kinetics of these processes. Intermetallic compounds and IMCs are produced commercially by conventional manufacturing methods. However, the method based on the principle of combustion synthesis appears to be promising for ease of production [7]. Studies on the combustion synthesis of intermetallic compounds have focused to a large extent on the NiAl and Ni<sub>3</sub>Al composites [8-16]. Intermetallic compounds, especially metal aluminides (such as nickel, titanium, cobalt, and niobium aluminides) have been considered as promising materials for high-temperature structural applications [17-20]. This is due to their physical and mechanical properties, which include low density, high specific strength, excellent creep resistance, and good oxidation and corrosion resistance. Conventional processing techniques used to fabricate

intermetallic compounds are generally through a combination of melting, casting, powder grinding, and consolidation by hot pressing. However, these techniques such as melting and casting methods are inapplicable to the fabrication of many intermetallic alloys due to, for example, a large difference between the melting points of constituent elements [21]. Nickel aluminized intermetallic compounds (NiAl and Ni<sub>3</sub>Al) have received considerable attention for high temperature structural and coating applications, for example, as heat shields for combustion chambers and as vanes in industrial gas turbines [19-21].

The interface of Ni-SiC particulates is thermodynamically unstable [22]. Hence, the combustion temperature is very important on dissolution rate of SiC in Ni matrix. Some studies were performed on the positive effects of the interfacial reactions on the mechanical properties of the Ni-SiC composites [23], and various studies were performed on the high-temperature strength of the Ni based composites reinforced by continuous or discontinuous ceramic particulates [24]. Among these studies, no attention has been given to the effect of dissolution rate of SiC on the working temperature behavior of SiC reinforced NiAl-Ni<sub>3</sub>Al intermetallics. In the present work, the combustion was applied for the fabrication of SiC added Ni<sub>3</sub>Al IMCs, and the objective is to investigate the effect of decomposition rate of initially added SiC particles on the working temperature of IMCs.

## 2. Experimental Procedure.

Commercial nickel (99% purity, 7µm average particle size), aluminum (99.8% purity, 10µm average particle size) and SiC (99% purity, 20µm average particle size) were used. The base powder compositions were prepared from 86.71 wt.%Ni and 13.28 wt.%Al. SiC powder was mixed

with the base powder at the ratios of 1, 3 and 5 vol.%. The intermetallic compound samples were obtained by reagent powder mixtures prepared according to the following operations for entire sample types. The powder compositions were mixed in an eccentric mixer for 20 min. After mixing, the powder mixtures were pressed to form a pellet in a cylindrical mould under an uniaxial pressure (300 MPa). Diameters of the compacts were 12 mm and heights were 10 mm. Subsequently, the compacts were placed into a vacuum tubular furnace and the combustion of the compacts was carried out at 600-700-800 °C in the argon atmosphere. Quantitative metallography was used for grain size determination, but it is often not accurate for determining relative amounts of particles or porosities by point counting. Therefore, density measurements were combined with the results of quantitative metallography to obtain the volume fraction of particles and porosities [25].

Microstructural evolution of the samples was investigated by optical and scanning electron microscope (SEM). Elemental analysis was carried out by using Tracor-Northern brand energy dispersive X-ray analyzer (EDX) attached to the SEM. Information about the variations of the hardness of the intermetallic phases were obtained by Vickers microhardness method ( $HV_{0.2}$ ), and the phase vol.% were determined by image analyzer. Phase analysis was carried out by the X-Ray Diffraction (XRD) via  $CuK_{\alpha}$ . Differential thermal analysis (DTA) was performed on an instrument fitted with a pair of matched alumina crucibles

with tantalum lids, and specimens were heated at 5 °C/min.

### 3. Results

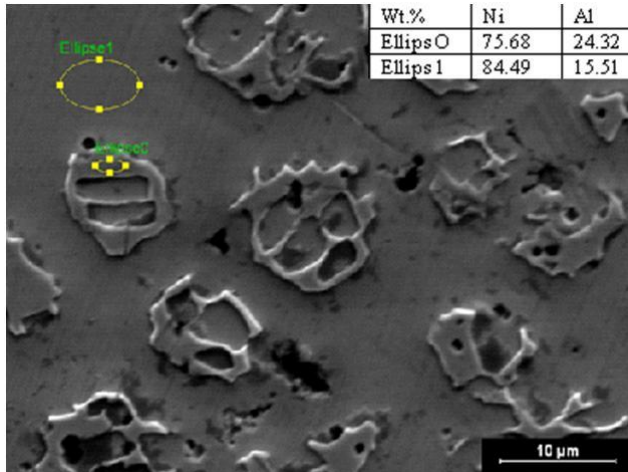
The production parameters of compact samples are listed in Table 1. During combustion, the exothermic reaction between nickel and aluminum powders generates enough heat to produce a liquid phase. This liquid provides a faster diffusion than encountered in the solid state leading to enhanced densification [26]. The amount of liquid phase formed depends on the powder composition (aluminum content) and temperature [26]. The application of high compact pressure before reaction sintering helps in eliminating the big pores often observed for samples compacted by low pressure. A pressure of 300 MPa is sufficient to obtain 99.9% dense compacts during the reaction synthesis of various intermetallics in the Ni-Al system [27-29]. Hence, the pressure was taken constant as 300 MPa. The SEM micrograph and XRD of sample S<sub>1</sub> were shown in Fig. 1a and Fig. 1b, respectively. It is seen that NiAl intermetallics were formed as particulate form in microstructure (Fig. 1a). Their concentrations were detected to be near to 5 vol.% (Table 2).

Table 1. Powder pressing and sintering parameters and reinforce ratios (wt.%)

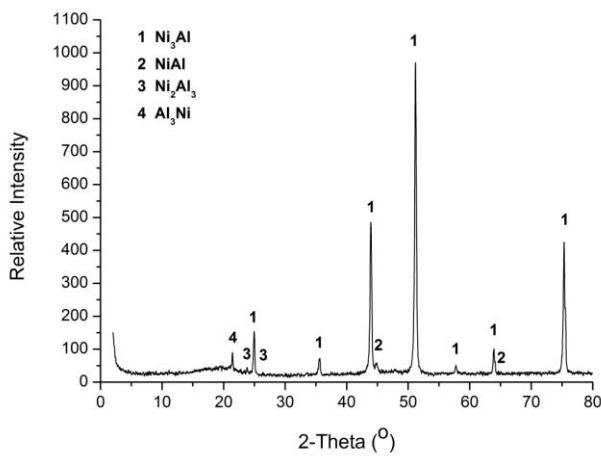
Sample. Num.	Compact. Pressure MPa	Combustion. Temp. °C	SiC Reinforcer. Vol.%
S1	300	600 °C	-
S2	300	600 °C	1
S3	300	600 °C	3
S4	300	600 °C	5
S5	300	700 °C	1
S6	300	800 °C	1
S7	300	800 °C	5

Table 2. Adiabatic temperature, microhardness, vol% and enthalpy of formation of phases.

Sample Num.	Combust. Temp. °C	Adiabatic Temperature °C	Ni <sub>3</sub> Al			NiAl	
			Microhard. (HV)	Grain size μm	Enthalpy J/mol	Microhard. (HV)	Vol.%
S1	600 °C	1381	968	40	1.2		4.7
S2	600 °C	1376	966	30	0.024	1052	12
S3	600 °C	1368	951	20	0.0034	1350	17
S4	600 °C	1345	964	10	0.00012	1263	23
S5	700 °C	1341	964	20	0.7	1246	16
S6	800 °C	1334	800	10	0.04	1368	19
S7	800 °C	1322	-	5	0.00008	1345	38



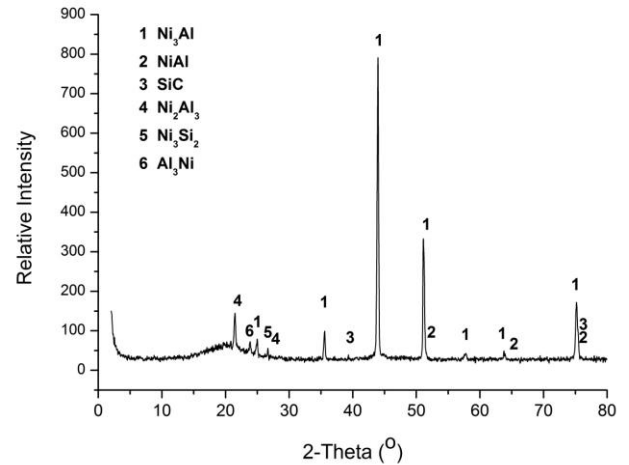
a



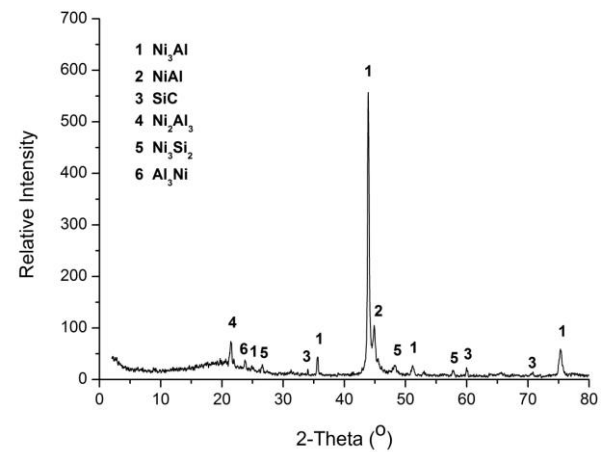
b

Fig. 1. a) SEM micrograph of sample *S*<sub>1</sub>, b) XRD pattern of sample *S*<sub>1</sub>.

Even though the pressure was high (300 MPa), the sintered compacts have small amount of porosity (Fig. 1a). The reason for the porosities may be due to the adsorbed gases and volatile impurities in the reactant powder mixtures. During synthesis, the released gaseous phases fill the pores and hinder complete densification. The high pressure cell is completely isolated from the atmosphere and the trapped gases cannot escape from the compact. XRD result shows that Ni<sub>3</sub>Al, NiAl, Ni<sub>2</sub>Al<sub>3</sub>, Al<sub>3</sub>Ni phases are present and the base phase is Ni<sub>3</sub>Al in sample *S*<sub>1</sub> (Fig 1b). SiC was added to the samples *S*<sub>2</sub>-*S*<sub>3</sub>-*S*<sub>4</sub> at the ratio of 1, 3 and 5 vol.%, respectively. XRD results of the samples *S*<sub>2</sub> and *S*<sub>4</sub> were given in Fig.2a and Fig.2b, respectively. It is seen from the figures that the samples contains especially Ni<sub>3</sub>Al, NiAl and SiC phases and other minor phases (Fig. 2a, 2b). It was detected from the metallographic examination and the XRD results that NiAl phase ratio increased from 4.7 to 23vol.% by the increase of the SiC reinforcement content to 5 vol.% (Table 2).



a

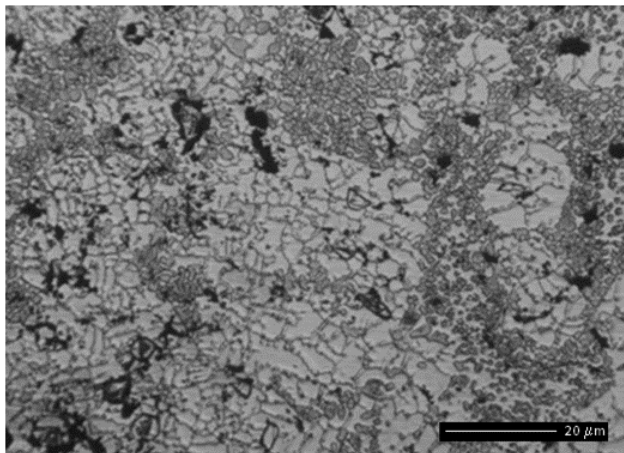


b

Fig. 2. XRD patterns obtained from a) sample *S*<sub>2</sub>, b) sample *S*<sub>4</sub>.

Optic micrographs of the samples *S*<sub>2</sub> and *S*<sub>4</sub> were given in Fig. 3a and Fig. 3b, respectively. The etching solution reacts faster with Ni<sub>3</sub>Al than either NiAl or Ni<sub>2</sub>Al<sub>3</sub>. That is why; the white phases or precipitate phases are NiAl, whereas the grey phase or the matrix is Ni<sub>3</sub>Al. The micrographs of all samples were shown that SiC particles were partially decomposed to the main matrix, and the size of SiC particles decreased. In addition, SiC is effective on the matrix grain size (Fig.3a-3b) by affecting formation temperature, formation enthalpy of intermetallic phases (Table 2). The SEM microstructure of the samples *S*<sub>4</sub> was shown in the Fig. 4. The reaction sintering of Ni<sub>3</sub>Al consists of a complex reaction with several sequential steps. First, the Al-rich compound NiAl<sub>3</sub> forms. Subsequently, this phase reacts with Ni to form NiAl. Depending on the availability of Ni in the vicinity of NiAl, Ni<sub>3</sub>Al may also form [28,29]. Therefore, in a reaction sintered compact where the reaction is incomplete, NiAl, Ni<sub>3</sub>Al intermetallic phases are likely to be present. EDS analysis were taken from

the points that were labeled in the microstructures were given in Fig. 4, where ‘Ellipse 0’ which occurred in intergranular form is NiAl, and ‘Rectangle 1’ is a pore formed after sintering (Fig. 4). The microstructure shows that SiC particulates partially or fully decomposed. From EDS analysis, we can see that C and Si atoms dissolved to all of the phases. Furthermore, the dissolution of these atoms changed the microstructure, and the increase of the SiC ratio affected the vol.% of Ni<sub>3</sub>Al phase (Table 2). On the change of microstructure dissolution of SiC can be attractive, because the presence of Si and C atoms decreases the chemical potential of the Ni<sub>3</sub>Al, and decreases the heat of formation of the NiAl system [30].



a

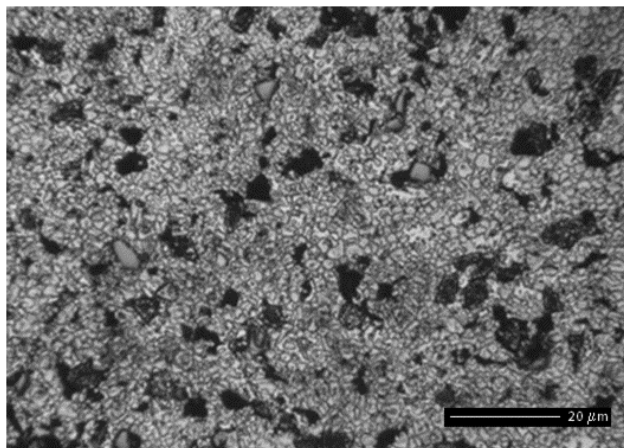


Fig. 3. Optical micrographs of the sample a) S<sub>2</sub>, b) S<sub>4</sub>, (Mag.5x15).

Stoichiometric Ni-Al composition can produce as much as 50 vol.% liquid phase when the sintering temperature is in the range of 600-700°C [24-27], hence the VCS temperature was increased gradually from 600 to 800 °C. The samples S<sub>5</sub>, S<sub>6</sub> and S<sub>7</sub> compacts were prepared at combustion temperatures of 600°C, 700°C and 800°C, respectively.

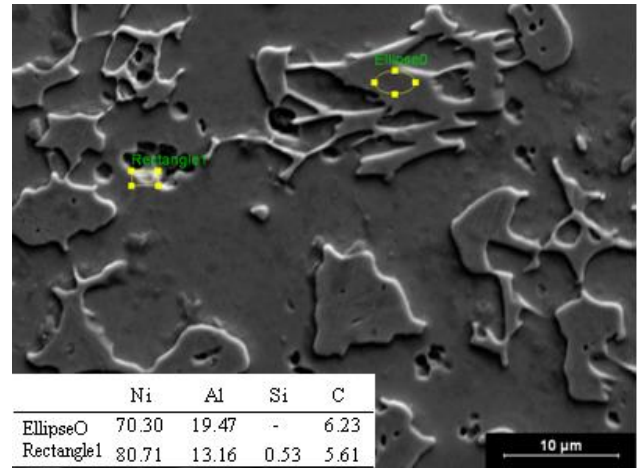


Fig. 4. SEM micrograph of the sample S<sub>4</sub>.

By comparing optic micrograph of samples S<sub>4</sub> and S<sub>5</sub>, it can be seen that the size of secondary phases at the grain boundaries of the sample S<sub>5</sub> were increased (Fig.5). SiC particles were dissolved due to the nature of the VCS process which exhibits exothermic reaction, and the temperature of the exothermic reaction reached to the dissolution temperature of the SiC reinforce particulates. The optical micrograph of the samples S<sub>6</sub> was shown in the Fig. 6. The size of secondary phase at the boundary of the crystallite and the pores increased (Fig. 6), and the size of the grains decreased by the increase of the combustion temperature. The increase of the SiC carbide reinforce ratio changed the dissolution rate and reactive reaction temperature. If the combustion temperature reaches the melting point of the aluminates and more, the evolution and entrapment of low melting point impurities or gaseous phase forms during the violent reactions [28]. For this reason, large pores can form due to local explosions in the compacts. The sample S<sub>7</sub> was sintered for 800 °C (Fig. 7a), and it is thought about the formation of the new formed microstructure that the melting of the Al-rich phase initiates the combustion. The combustion reactions involve definite interaction of solid Ni with Al-rich liquid. Reaction diffusion model is the one that is most commonly used to describe this kind of interaction. In that case, the product layer grows due to mass transport and the growth is unrelated to the dissolution of the layer. An example of this can be found in isothermal dissolution of Ni in unsaturated liquid Al where intermetallic layer, Al<sub>3</sub>Ni forms up to a temperature of 800 °C [28]. The first layer that forms due to the solid-liquid interaction contains Al<sub>3</sub>Ni. Simultaneously, the temperature also increases continuously and leads to progressive dissolution of the layer. When it reaches 800 °C, Al<sub>3</sub>Ni starts melting. The Al<sub>3</sub>Ni layer, which is now in contact with the Ni particle, gives rise to phases richer in Ni. More importantly, microstructures have revealed one common reaction mechanism that is operative in VCS of NiAl. This common reaction mechanism is found to be very close to the one proposed in [27]. From the SEM microstructure (Fig. 7a) and XRD (Fig. 7b) of S<sub>7</sub>, the dissolution of the

SiC carbides can be seen clearly in sequence. In VCS, the heat loss in the reaction zone by conduction is high leading to incomplete reaction. Hence, for combustion temperature of 600 °C (Fig. 4), the dissolute SiC carbide having unsolved SiC portion at the center are present, and for 800 °C (Fig. 7a) some fully solvated SiC carbides can be seen. The diffusion rate of the Si atom from SiC to Ni matrix is higher than the diffusion rate of Ni and Al atoms from matrix to SiC [26], hence pores occurred at dissolved SiC carbides due to Kirkendal effect. From XRD patterns (Fig. 7b) also it was seen that the undissolved SiC carbide ratio for sample S<sub>7</sub> was decreased, and the ratio of NiAl intermetallics was increased.

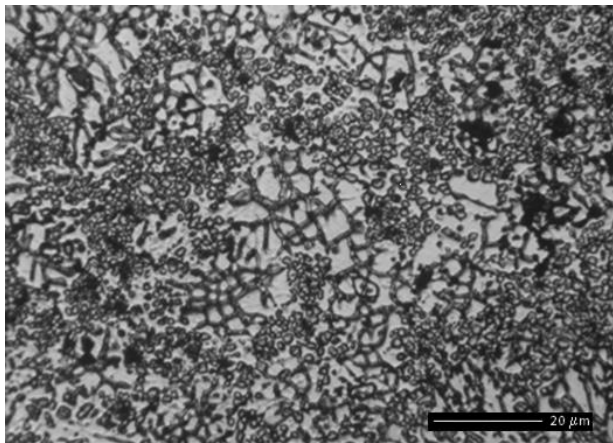


Fig. 5. Optic micrograph of the sample S<sub>5</sub>.

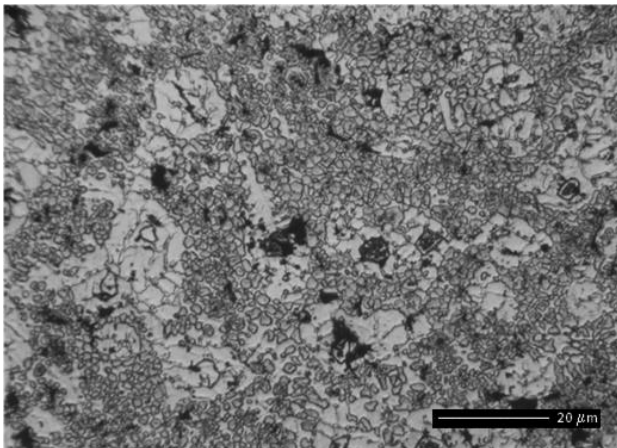
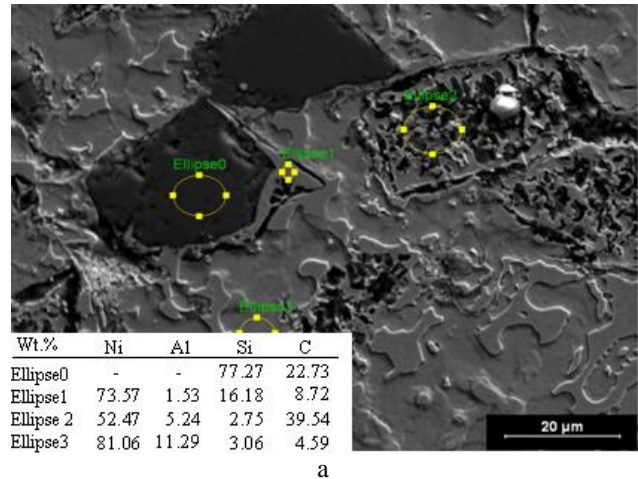
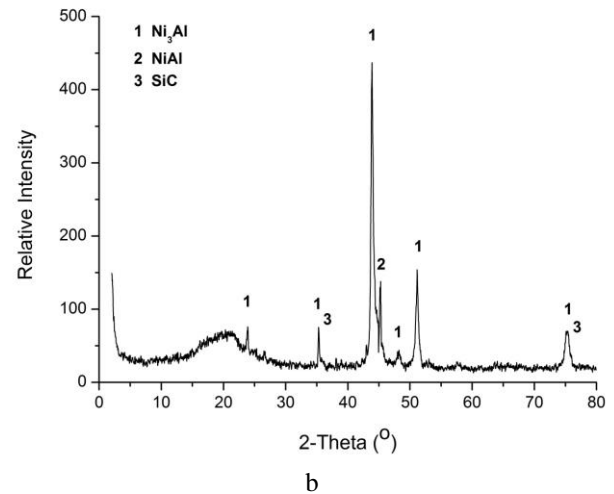


Fig. 6. Optic micrograph of the samples S<sub>6</sub>.

The microhardnesses of the SiC-NiAl composites prepared by VCS are listed in Table 2. The hardness values of the VCS compacts are higher than that of the NiAl reported by Cheng et al [22]. The difference between hardness values are thought to be due to high internal stress. The compact samples contain approximately 1-3 vol.% porosity. The porosity vol.% of samples were not change significantly either on increasing the sintering temperature or on decreasing the amount of matrix NiAl phase.



a



b

Fig. 7. a) SEM micrograph of the sample micrograph of the sample, b) XRD of the sample S<sub>7</sub>.

#### 4. Discussion

The densification mechanism in SiC-NiAl composites may be different from that in pure NiAl. The minor volume fraction in the SiC-NiAl composites is undissolved SiC phase. During pressurization, the densification takes place by the dissolution of the SiC particles. The yield strength of Ni and Al being very low as compared to that of SiC, these ductile phases deform significantly and fill the voids. On raising the temperature, the reaction starts and a liquid phase forms. The volume fraction of the liquid phase decreases with the progress of the reaction. Finally, the liquid disappears when the reaction is complete. However, the presence of the liquid even for a short period is beneficial for densification, as second stage of particle rearrangement takes place during this period. In the SiC-NiAl composites, the volume fraction of liquid phase and the heat generated due to reaction are less as compared to the pure NiAl. Consequently, the time required for densification is longer. When the volume fraction of the matrix phase is

low, the amount of liquid phase is not sufficient to fill all the pores (Fig.3 and 6). The XRD patterns (Fig. 2b, Fig. 7b) indicate that the composites contain mainly SiC, NiAl and Ni<sub>3</sub>Al phases. Irrespective of the composition and the synthesis temperature, all the compacts have similar microstructures. Increase in the sintering temperature from 600 to 700 °C results in a better bonding between the matrix and the SiC carbides leading to the improvement in mechanical microhardness. Further increase in temperature to 800 °C caused grain growth in the matrix phase which may result in deterioration of the toughness. In VCS, fully dense compacts were obtained when the combustion temperature (700 °C) was maintained for 15 min. In case of composites under high combustion temperature, the vol.% NiAl was increased up to 38 vol.%. On this ratio, the effect of the SiC addition is apparent. The temperature reached after combustion (1680°C) is higher than the melting points of all the intermetallics in the Ni-Al system. This results in the formation of a liquid phase, and the densification proceeds through liquid phase sintering. The time required for complete densification depends on the volume fraction of the liquid phase. It increases with the decrease in the volume fraction of the liquid phase forming additives. On the XRD patterns of the SiC-NiAl samples, no elemental Ni or Al was seen. However, as comparison of the samples, the concentration of NiAl was changed (Table 2). The formation of the liquid during VCS enhances the reaction between SiC and the other constituents of the composites. A part of carbon atoms may be dissolved in Ni<sub>3</sub>Al phases. The microstructures consist of equiaxed grains of SiC in the matrix of Ni<sub>3</sub>Al intermetallics (Fig.3and 4).

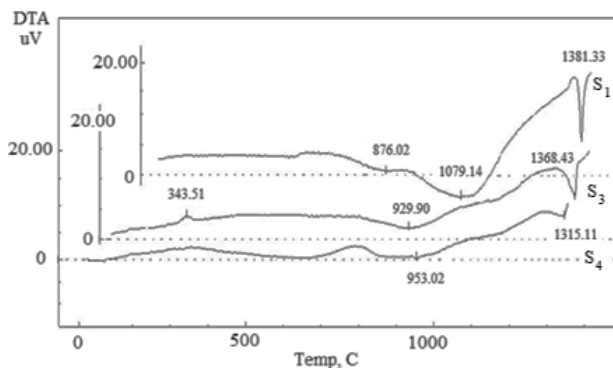
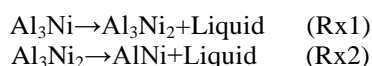


Fig. 8. DTA curves showing the reactions taking place during heating of sample S<sub>1</sub>, S<sub>2</sub> and S<sub>4</sub>

DTA results of the samples S<sub>1</sub>, S<sub>3</sub> and S<sub>4</sub> that is showing the effect of SiC reinforce on the reaction temperatures, formation enthalpies of Ni<sub>3</sub>Al, and vol.% of AlNi were given in Fig. 8. The peaks of curves specify the reaction temperatures, and areas under the curves indicate the enthalpy of formation reactions. For sample S<sub>1</sub>, three essential reactions were seen by heating up to 1400 °C.



In a reaction-sintered compact, four intermetallic phases (Ni<sub>3</sub>Al, NiAl, Al<sub>3</sub>Ni, Al<sub>3</sub>Ni<sub>2</sub>) are likely to be present [30]. The temperature of Rx1 is important for the real working temperature of the intermetallics in industrial applications. In other words, the increase of the dissolution temperature of the Rx1 is extremely important for the intermetallics working at high temperatures. The decomposition temperature of the Rx1 was increased approximately 80 °C for sample S<sub>4</sub> by 5wt.% SiC addition. We have not seen Rx2 for sample S<sub>3</sub> and S<sub>4</sub>. This means that probably the concentration of Al<sub>3</sub>Ni phase is too small for sample S<sub>2</sub> and S<sub>3</sub>. The presence of the Al<sub>3</sub>Ni phase is not wanted in Ni<sub>3</sub>Al intermetallics working at high temperatures [30, 31]. For this reason, it seems that the addition of SiC reinforce is effective on the repressing the formation of the Al<sub>3</sub>Ni phase. The decomposition temperature of the Rx3 was decreased from 1381 to 1315 °C by SiC addition, and the formation enthalpy of Al<sub>3</sub>Ni intermetallics was decreased from 1.2 to 0.00012 J/K-Mol (Table 2). The areas under the DTA curves for Rx3 of the sample S<sub>3</sub> and S<sub>4</sub> are consistently smaller than that of the reference sample S<sub>1</sub>. There may be several thermodynamic and kinetic reasons for this behavior. One possible explanation for this variation is that the Ni and Al content in the NiAl<sub>3</sub> and the matrix are different for these two intermetallic samples. In sample S<sub>1</sub>, the Ni<sub>3</sub>Al intermetallic contains more Ni than that in sample S<sub>3</sub> and S<sub>4</sub> (Fig.1, Fig.4, Fig.7). The free energy of formation for Ni<sub>3</sub>Al increases as the Ni content of the intermetallic increases at 1380 °C [31]. If this trend holds at higher temperatures, the difference between the DTA curves from sample S<sub>1</sub>, S<sub>3</sub> and S<sub>4</sub> intermetallics may be at least partially explained by the difference in Ni content of the intermetallics. However, this decrease in the heat released due to the increase in Ni content must also be counteracted to some degree by the decrease in the volume fraction of Ni<sub>3</sub>Al intermetallics. It was counted from microstructure micrographs that AlNi concentration was increased by SiC addition. The increase of AlNi intermetallic ratio is an expected result and it was preferentially wanted for industrial applications. A similar argument may also be valid for the latent heat released during the formation of AlNi phase. As a result, the features observed in the heating DTA curves (Fig. 8) may be used to design the final macrostructure of the intermetallics. In this respect, three important features of the DTA curves in Fig. 8 are;

- (1) The broadness of the AlNi<sub>3</sub> dissolution reaction during heating, indicating slow dissolution reaction during kinetics;
- (2) The temperature difference between the high temperature end of the Rx1 and Rx3 dissolution curve during heating;
- (3) The elimination of Al<sub>3</sub>Ni<sub>2</sub> phase;
- (4) The increase of AlNi phase ratio for samples having SiC reinforce.

## 5. Conclusion

The grain size of the samples having 5 wt.% SiC are finer than the samples having 1 wt.% SiC reinforce (Table 2). For the samples having 1 wt.% SiC reinforce rate, almost all of the SiC particles were dissolved to the main intermetallic Ni<sub>3</sub>Al phase, however SiC particles were partially dissolved at the sample having 5 wt.% SiC reinforce. The increase of the SiC carbide reinforce particulates ratio changes the dissolution rate and reactive reaction temperature. The melting of the Al-rich phase initiates the combustion of the new formed microstructure, and the combustion reactions involve definite interaction of solid Ni with Al-rich liquid.

During sintering and dissolution of SiC, C and Si atoms dissolved to all of the phases, and the dissolution of these atoms changed the microstructure. Depending on Si concentration, the dissolution temperature of Al<sub>3</sub>Ni phase was increased, and Al<sub>3</sub>Ni<sub>2</sub> phase was not seen in the structure. The increase of the SiC reinforce ratio decreases Ni<sub>3</sub>Al phase vol.%. The intergranular phase is NiAl, and the matrix phase is Ni<sub>3</sub>Al. The size of secondary phase at the grain boundaries and the pores increased and the size of the grains decreased with sintering temperature. The melting of the Al-rich phase initiates the combustion of the new formed microstructure, and the combustion reactions involve definite interaction of solid Ni with Al-rich liquid. Depending on the sintering temperature, more or less molten NiAl and Ni<sub>3</sub>Al phase can form. The variation of sintering temperature effects the transient liquid phase formation, value of combustion temperature, melt fraction of the product and overall densification.

## References

- [1] Z.A. Munir, U. A. Tamburini, *Mat. Sci. Rep.* **3**, 277 (1989).
- [2] A.G. Merzhanov, *J. Mater Process Tech.* **56**, 222 (1996).
- [3] D. Zhong, J. J. Moore, J. Disam, S. Thiel, I. Dahan, *Surf. Coat. Tech.* **120**, 22 (1999).
- [4] P. Mossino, F.A. Deorsola, D. Vallauri, I. Amato, *Ceram. Inter.* **30**, 2229 (2004).
- [5] J.D. Walton, N.E. Poulos, *J. Am. Ceram Soc.* **42**, 40 (1959).
- [6] S.D. Dunmead, Z.A. Munir, J.B. Holt, D.D. Kingman, *J. Mater Sci.* **26**, 2410 (1991).
- [7] S. Murali, T. Sritharan, P. Hing, *Intermet.* **11**, 279 (2003).
- [8] K. Morsi, *Mat. Sci. Eng. A.* **299**, 1 (2001).
- [9] Y. Jiang, C. Deng, Y. He, Y. Zhao, N. Xu, J. Zou, B. Huang, C.T. Liu, *Mat. Lett.* **63**, 22 (2009).
- [10] A. Biswas, S. K. Roy, *Acta Mat.* **52**, 257 (2004).
- [11] A.S. Rogachev, V.A. Shugaev, C.R. Kachelmyer, A. Varma, *Chem. Eng. Sci.* **49**, 4949 (1994).
- [12] A. Hibino, S. Matsuoka, M. Kiuchi, *J. Mat. Process Tech.* **112**, 127 (2001).
- [13] R. Orru, G. Cao, Z.A. Munir, *Chem. Eng Sci.* **54**, 3349 (1999).
- [14] E.G. Kandalova, V.I. Nikitin, J. Wanqi, A.G. Makarenko, *Mat. Lett.* **54**, 131 (2002).
- [15] N. Bertolino, M. Monagheddu, A. Tacca, P. Giuliani, C. Zanotti, U. A. Tamburini, *Intermet.* **11**, 41 (2003).
- [16] V. Gauthier, F. Bernard, E. Gaffet, C. Josse, J.P. Larpin, *Mater. Sci. Eng. A.* **272**, 334 (1999).
- [17] M.N. Mungole, R. Balasubramaniam, A. Ghosh, *Intermet.* **8**, 717 (2000).
- [18] B.M. Warnes, N.S. DuShane, J.E. Cockerill, *Surf.Coat. Tech.* **148**, 163 (2001).
- [19] V. Gauthier, F. Bernard, E. Gaffet, D. Vrel, M. Gailhanou, J.P. Larpin, *Intermet.* **10**, 377 (2002).
- [20] C. Nishimura, C.T. Liu, *Scr. Metall. Mater.* **26**, 381 (1992).
- [21] F. Scheppe, P.R. Sahm, W. Hermann, U. Paul, J. Preuhs, *Mat. Sci. Eng. A.* **329**, 596 (2002).
- [22] K. Bhanumurthy, R. Schmid-fetzer, *Compos part A-Appl S.* **32**(3-4), 569 (2001).
- [23] G. Fei, L. Jinjun, L. Weimin, *Compos. Sci. and Technol.* **68**, 566 (2008).
- [24] D. B., Lee, J. K., *Deug, Intermetallic*, **9**, 51 (2001).
- [25] O. Yilmaz, S. Buytoz, *Compos. Sci. Technol.*, **61**, 2381 (2001).
- [26] S. C. Tjong, Z.Y. Ma, *Mat. Sci. Eng. A* **29**, 49 (2000).
- [27] S. Miura, Y. Mishima, in: Horton. J.A., Baker, I., Hanada, S., Noebe, R.D., Schwartz, D.S. (Eds.), *High Temperature Ordered Intermetallic Alloys VI*, Boston, MA, 1995, pp. 561.
- [28] K.H. Wu, C.T. Liu, in: Baker, I., Darolia, R., Whitten, J.D., Berger, M.H. Yoo (Eds.), *High Temperature Ordered Inter-metallic Alloys V*, MRS, Pittsburgh, PA, 1993, pp. 841.
- [29] Z.A. Munir, *Self-propagating High-temperature Synthesis*, *Encyclopedia of Materials: Science and Technology*, Elsevier, USA, 2008, pp. 8323.
- [30] A. Hibino, S. Matsuoka, M. Kiuchi, *J. Mater. Proc. Tech.* **112**, 127 (2001).
- [31] H. Xue, Munir, Z. A., *J. Europ Ceram. Soc.* **17**, 1787 (1997).
- [32] A. Biswas, S. K. Roy, K.R. Gurumurthy, N. Prabhu, S. Banerjee, *Acta Mat.* **50**, 757 (2002).

\*Corresponding author: oguler@firat.edu.tr